Draft version May 21, 2018
Typeset using LaTeX **preprint2** style in AASTeX62

Rotating Stars from *Kepler* Observed with Gaia DR2

James. R. A. Davenport[1,2,*] and Kevin R. Covey[1]

[1]*Department of Physics & Astronomy, Western Washington University, 516 High St., Bellingham, WA 98225, USA*
[2]*Department of Astronomy, University of Washington, Seattle, WA 98195, USA*

ABSTRACT

We have matched the astrometric data from *Gaia* Data Release 2 to the sample of stars with measured rotation periods from *Kepler*. Using 30,305 stars with good distance estimates, we select 16,248 as being likely main sequence single stars within a 0.5 mag region about a 1 Gyr isochrone. This removes sub-giants and unresolved binary stars from the sample. The rotation period bimodality, originally discovered by McQuillan et al. (2013), is recovered for stars out to 525pc, but is not detectable at further distances. We also find a significant width in the stellar main sequence of M_G ~0.25 mag, as well as a increase in the average rotation period correlated with the M_G offset at a given color (mass). We interpret this to be the measurable change in luminosity and loss of angular momentum as stars evolve along the main sequence, which may provide a new independent test of stellar evolution and gyrochronlogy models. This investigation represents the first step in understanding the star formation history of our solar neighborhood as traced through stellar angular momentum loss.

1. INTRODUCTION

The *Kepler* mission (Borucki et al. 2010) a new era for enabling detailed study of angular momentum loss in low-mass stars. long noted as a means to possibly age-date stars (gyro), open clusters give hope that this general model works for low-mass stars many Qs exist about details. these include Qs about initial rotation period distribution (e.g. Barnes 2010; Matt et al. 2015), the specific prescription for spin-down (Angus et al. 2015), and exploring the efficiency of this angular momentum loss mechanism at old ages (van Saders et al. 2016).

Corresponding author: James. R. A. Davenport
James.Davenport@wwu.edu

* NSF Astronomy and Astrophysics Postdoctoral Fellow DIRAC Fellow

one of the most compelling results from the rotation work in *Kepler* is the discovery of a period bimodality. McQuillan et al. (2013) found bimodal feature, in M and later K stars (McQuillan et al. 2014). Davenport used Gaia DR1 to remove contamination from sub-giants and found the feature in G dwarfs. this feature proposed to be either a new short-lived transition or instability phase of momentum loss, or a signature of star formation history imprinted in the present-day rotation period distribution. However, to date this feature has only been observed in the *Kepler* rotation period catalog, and most critically only for stars within ~300 pc.

In this letter we follow the work of Davenport (2017) in studying the *Kepler* rotation period sample using astrometric data from the *Gaia* mission (Gaia Collaboration et al. 2016). By matching the McQuillan et al. (2014) rotation period catalog to the newest data from *Gaia* Data Release 2 (Gaia Collaboration et al. 2018), we can use precise distances for essentially every star to select likely main sequence dwarfs to distances well over 1 kpc. Importantly this filters out both sub-giants (the main contaminant noted by Davenport (2017)), and unresolved binary stars. Here we demonstrate the power of such a combined time-domain and astrometric sample for constraining the detailed evolution of main sequence stars themselves, and exploring the star formation history of the Milky Way.

2. THE *Kepler*–GAIA DATA

We used the largest homogeneous catalog of rotation periods available from the *Kepler* mission. The sample from McQuillan et al. (2014) provides rotation periods for more 34,030 stars, measured using the Auto-Correlation Function (ACF). While the ACF does not have as fine of resolution in recovering periods as compared with methods such as the Lomb-Scargle Periodogram, it is more robust to detecting the true period as opposed to an alias, and more complete for batch analysis of all stars (e.g. see Aigrain et al. 2015).

The *Kepler* data was matched to the *Gaia* DR2 source catalog using a 1 arcsecond radius. We used the *Kepler*–Gaia cross-match made publicly available by M. Bedell, which included entries for 195,830 sources. *Kepler*-based stellar parameters included in this cross-match come the Data Release 25 *Kepler* catalog. Joining this cross-matched table to the McQuillan et al. (2014) catalog, we found 33,538 sources.

To select stars with good parallaxes, as well as high quality photometry from *Gaia*, we selected stars with the following criteria:

- Parallax error < 0.1 mas
- $\sigma(M_G)/M_G < 0.01$
- $\sigma(G_{BP})/G_{BP} < 0.01$
- $\sigma(G_{RP})/G_{RP} < 0.01$

Rather than simply use the inverse *Gaia* parallax values to measure the distance to sources, we use the improved distance prescription from Bailer-Jones et al. (2018), who provided independent distances estimates for 1.33 billion *Gaia* sources using a weak prior on the distribution of stars in our galaxy. We follow their suggested use of the distance catalog, we only include sources with `modality_flag` == 1 (i.e. not a bimodal distance solution) and `result_flag` == 1 (i.e. well constrained distance).

Our final sample contained 30,305 stars in Gaia DR2 with measured *Kepler* rotation periods that passed these selection criteria. A color–magnitude diagram of this sample is presented in Figure 1, with points colored by their rotation periods.

3. SELECTING MAIN SEQUENCE STARS

As in Davenport (2017), the color–magnitude diagram in Figure 1 shows many of the bluer stars in the McQuillan et al. (2014) sample are located significantly above the main sequence. These are likely subgiant stars, which do not follow the main sequence stars spin-down evolution (e.g. do Nascimento et al. 2012; van Saders & Pinsonneault 2013). Since Davenport (2017) found subgiants could obscure the rotation period bimodality for G dwarfs, these must be excluded from our analysis, but we encourage future studies to explore the wealth of angular momentum evolution data from these most-main sequence objects.

Beyond the subgiant contamination, we also see a secondary population of stars in a parallel track ∼0.75 mag above the normal main sequence, which are attributed to unresolved binary star systems. This pile-up above the main sequence occurs due to unresolved equal-mass (or nearly equal-mass) field binaries, and was seen in the *Gaia* DR1 data as well (Anderson

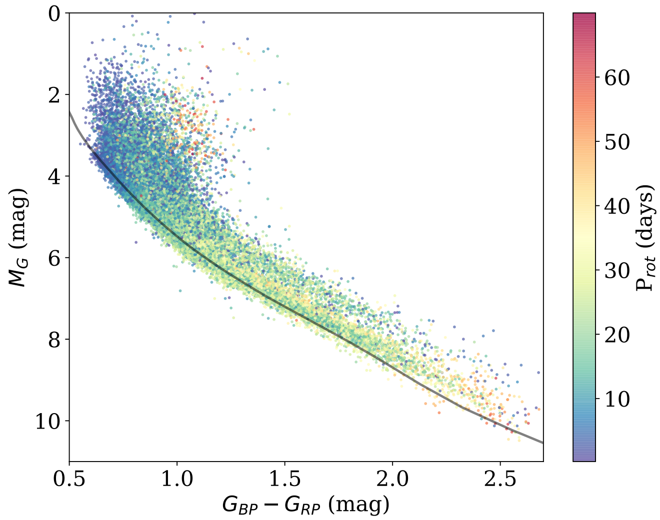

Figure 1. Color–magnitude diagram for 30,305 *Kepler* stars from the McQuillan et al. (2014) sample that are included in Gaia DR2, colored by their measured rotation period. For reference we show a 10^9 year MIST isochrone (black line) used to select likely main sequence, single stars (black line). A track of binary stars is apparent ∼0.75 mag above the main sequence. As in Davenport (2017), we find significant contamination of the rotation period sample for bluer stars by sub-giants.

et al. 2017). Since these systems may have experienced tidal evolution that could significantly impact their rotation evolution (e.g. Lurie et al. 2017), we must also remove these from our analysis. Though we do not explore the binary population in any detail here, this sample (perhaps with radial velocity follow-up) may provide useful insight into the tidal evolution of binary stars, and are good targets for characterizing binary star system properties. We also note a small number of systems above the even the equal-mass binary main sequence track, which could be due to unresolved triple star systems.

We use an isochrone from the Mesa Isochrones and Stellar Tracks suite (MIST; Choi et al. 2016) to choose likely main sequence stars in Figure 1. Our favored model to represent the main sequence in this study had [Fe/H] = +0.25 and an age of 10^9 years, and was chosen by-hand. Single, main sequence stars were selected in a region spanning 0.1 mag fainter and 0.4 mag brighter than the MIST isochrone, resulting in a final sample of 16,248 stars for analysis of their rotation period distributions.

4. TRACING THE PERIOD BIMODALITY

all the color–period diagrams vs distance:

re-define gyrochrone in terms of subtract 600myr gyrochrone off again, as in D17

these distance bins reach approximate distances above the galactic midplane of ∼60 pc in the nearest bin, to nearly 800 pc in the furthest bin, therefore spanning a large range in apparent age and possible star formation history

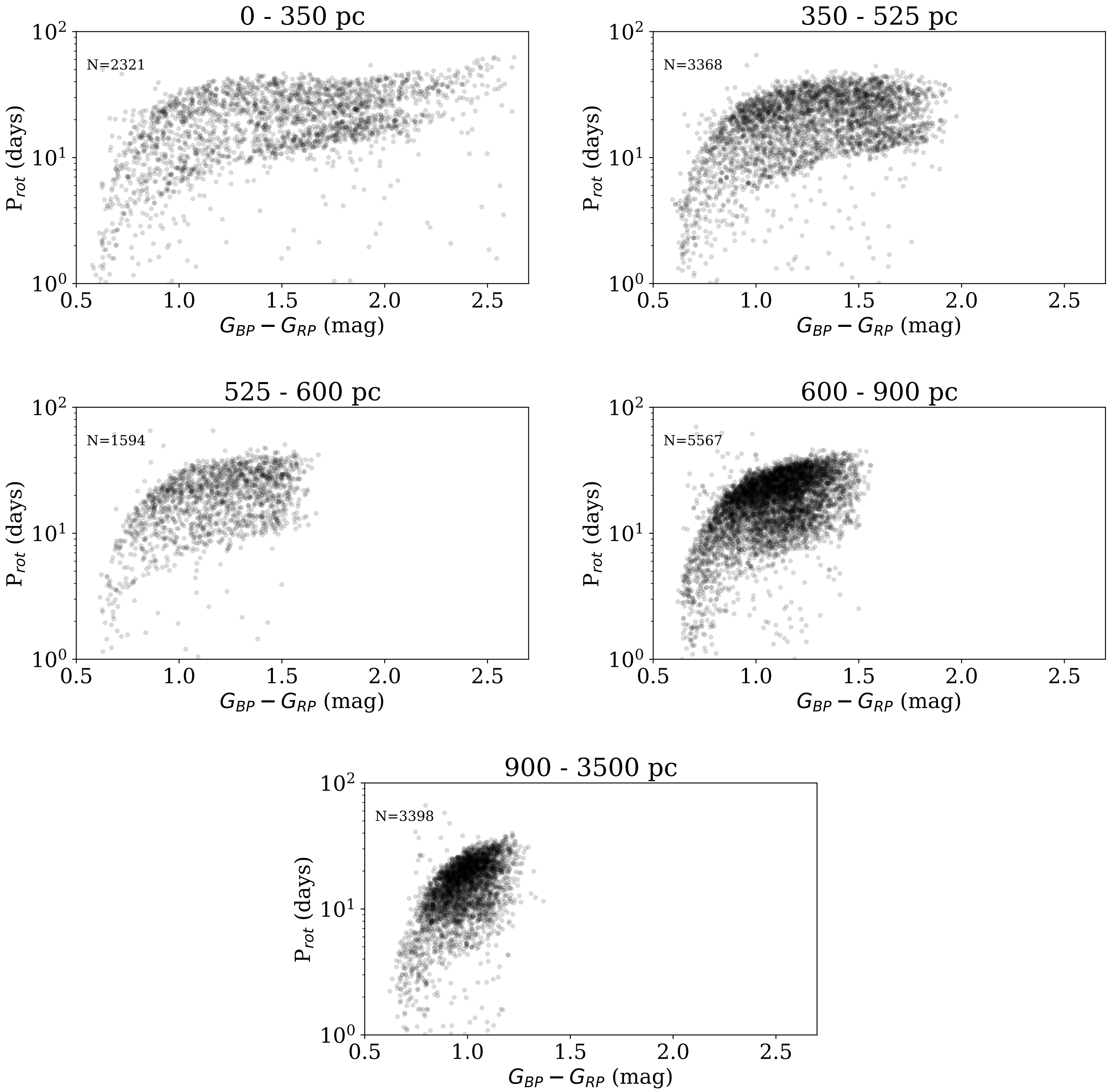

Figure 2. Color–period diagrams for our sample of likely main sequence stars, divided into bins of distance. Our nearest bin (within 350pc) is effectively the distance analyzed in Davenport (2017) using Gaia DR1, and clearly shows the rotation period bimodality for the entire sample. The brighter magnitude limit of the *Kepler* sample results in redder (fainter) stars missing in our further distance bins. The rotation period bimodality can be seen in the 350-525 pc bin, but is not found in the bluer stars at further distances.

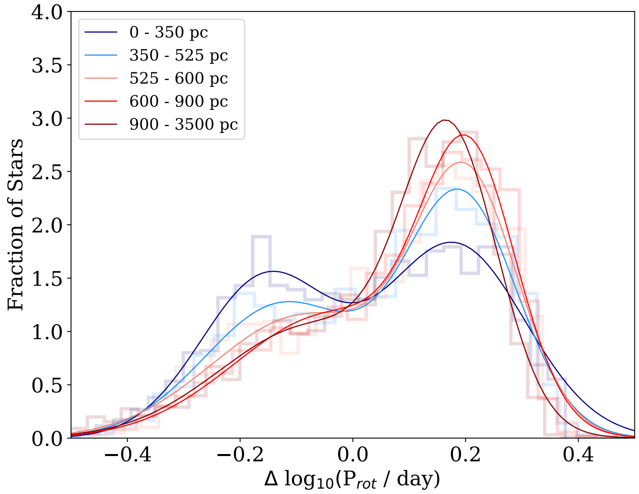

Figure 3. Histograms of the log rotation periods after a 600 Myr gyrochrone was subtracted for stars in the same five distance bins shown in Figure 2. The period bimodality for stars within 350 pc has two peaks similar to those found in Davenport (2017), at -0.15 and +0.18 dex. The fast rotating peak (left side) declines sharply at further distances, however.

5. RECALIBRATING STELLAR EVOLUTION MODELS

A subtle feature that we noticed in Figure 1 is the apparent color gradient (i.e. rotation period gradient) between the single and binary star main sequence populations. In Figure 1 this appears as a yellow stripe (i.e. rotation periods of 30-40 days) between these blue-green sequences for systems with colors of $G_{BP} - G_{RP} \approx 1.5$. To exaggerate this feature, we have reproduced a portion of our color–magnitude diagram focused on the main sequence near this stellar color in the left panel of Figure 4. A clear color gradient is present, with red points (slower rotators) appearing preferentially above the main sequence. The right panel of Figure 4 concretely demonstrates a correlation between the measured rotation period and the vertical offset (i.e. absolute magnitude) from the 10^9 year MIST isochrone. Slower rotating stars are apparently brighter at a given stellar color.

We interpret this observation as being due to the increase in luminosity of stars across their main sequence lives, coupled with the angular momentum loss that underpins gyrochronology. Indeed, the sequence of MIST isochrones shown in Figure 4 with ages of 10^8, 10^9, and 10^10 years clearly predicts an increase in brightness of the main sequence over time.

indeed, 0.7solarmass star traced over its life in both panels doesnt quite make sense. inverting CMD into precise ages w/ Gaia beyond scope of this work, but this figure suggests the MS is too wide given a reasonable age range. consider: younger stars, presumably more metal rich, should be redder, moving in the wrong direction to the affect we see here. more stellar masses and careful work needed... vertical spread in this parameter space is OK for a star, but maybe some color impact we not considering.... hmm.

however, looking at 0.7M period vs lum evolution, we see that the period seems to also drop off too rapidly compared to a model. combining the MM09 spin-down formulae for a 0.7M star, with the MIST isochrone evolution, we see the period range should go out to 60–80 days to get the right amplitude offset. That implies that at a given age (or vertical offset), the stars are rotating *faster* than expected. this is similar to the broken spin-down model suggested by (van Saders et al. 2016), and is potentially the first confirmation of this observation.

6. DISCUSSION

JRAD is supported by an NSF Astronomy and Astrophysics Postdoctoral Fellowship under award AST-1501418.

This work made use of the gaia-kepler.fun crossmatch database, created by Megan Bedell.

This project was developed as part of the 2018 NYC Gaia Sprint, hosted by the Center for Computational Astrophysics at the Simons Foundation in New York City.

This work has made use of data from the European Space Agency (ESA) mission *Gaia* (https://www.cosmos.esa.int/gaia), processed by the *Gaia* Data Processing and Analysis Consortium (DPAC, https://www.cosmos.esa.int/web/gaia/dpac/consortium). Funding for the DPAC has been provided by national institutions, in particular the institutions participating in the *Gaia* Multilateral Agreement.

REFERENCES

Aigrain, S., Llama, J., Ceillier, T., et al. 2015, MNRAS, 450, 3211, doi: 10.1093/mnras/stv853

Anderson, L., Hogg, D. W., Leistedt, B., Price-Whelan, A. M., & Bovy, J. 2017, ArXiv e-prints. https://arxiv.org/abs/1706.05055

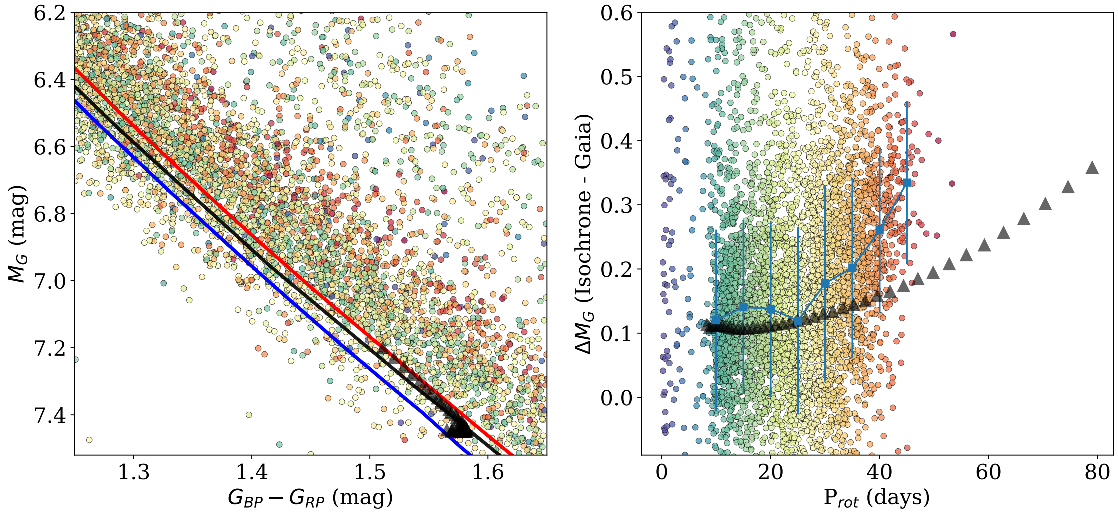

Figure 4. Left: Enlarged portion of the color–magnitude diagram from Figure 1 in a region centered near $\sim$0.75 $M_\odot$, with stars are colored by their measured *Kepler* rotation periods from McQuillan et al. (2014). MIST isochrones at ages of 10^8, 10^9, and 10^10 yr are shown for comparison (blue, black, and red lines). The predicted evolution of a 0.7 $M_\odot$ star is highlighted (black triangles). Right: Difference in M_G from the 10^9 yr MIST isochrone as a function of rotation period (point color again indicates rotation period, as in Left panel). Blue squares show an increase in the median M_G offset in bins of increasing rotation period. Error bars shown are the standard deviation of ΔM_G in each bin. The 0.7 $M_\odot$ star brightness evolution is shown as a function of rotation evolution from Meibom et al. (2009) (black triangles).

Angus, R., Aigrain, S., Foreman-Mackey, D., & McQuillan, A. 2015, MNRAS, 450, 1787, doi: 10.1093/mnras/stv423

Bailer-Jones, C. A. L., Rybizki, J., Fouesneau, M., Mantelet, G., & Andrae, R. 2018, ArXiv e-prints. https://arxiv.org/abs/1804.10121

Barnes, S. A. 2010, ApJ, 722, 222, doi: 10.1088/0004-637X/722/1/222

Borucki, W. J., Koch, D., Basri, G., et al. 2010, Science, 327, 977, doi: 10.1126/science.1185402

Choi, J., Dotter, A., Conroy, C., et al. 2016, ApJ, 823, 102, doi: 10.3847/0004-637X/823/2/102

Davenport, J. R. A. 2017, ApJ, 835, 16, doi: 10.3847/1538-4357/835/1/16

do Nascimento, J.-D., da Costa, J. S., & Castro, M. 2012, A&A, 548, L1, doi: 10.1051/0004-6361/201219791

Gaia Collaboration, Brown, A. G. A., Vallenari, A., et al. 2018, ArXiv e-prints. https://arxiv.org/abs/1804.09365

Gaia Collaboration, Prusti, T., de Bruijne, J. H. J., et al. 2016, A&A, 595, A1, doi: 10.1051/0004-6361/201629272

Lurie, J. C., Vyhmeister, K., Hawley, S. L., et al. 2017, AJ, 154, 250, doi: 10.3847/1538-3881/aa974d

Matt, S. P., Brun, A. S., Baraffe, I., Bouvier, J., & Chabrier, G. 2015, ApJL, 799, L23, doi: 10.1088/2041-8205/799/2/L23

McQuillan, A., Aigrain, S., & Mazeh, T. 2013, MNRAS, 432, 1203, doi: 10.1093/mnras/stt536

McQuillan, A., Mazeh, T., & Aigrain, S. 2014, ApJS, 211, 24, doi: 10.1088/0067-0049/211/2/24

Meibom, S., Mathieu, R. D., & Stassun, K. G. 2009, ApJ, 695, 679, doi: 10.1088/0004-637X/695/1/679

van Saders, J. L., Ceillier, T., Metcalfe, T. S., et al. 2016, Nature, 529, 181, doi: 10.1038/nature16168

van Saders, J. L., & Pinsonneault, M. H. 2013, ApJ, 776, 67, doi: 10.1088/0004-637X/776/2/67